Electronic Supplementary Material (ESI) for Nanoscale.

Supporting Information

Flexible Pressure Sensor Based on rGO/Polyaniline Wrapped Sponge with Tunable Sensitivity for Human Motions Detection

Gang Ge,[a] Yichen Cai,[a] Qiuchun Dong,[a] Yizhou Zhang,[a] Wei Huang,[a,b] Jinjun Shao,[a*]

Xiaochen Dong[a,c*]

[a]Key Laboratory of Flexible Electronics (KLOFE) & Institute of Advanced Materials (IAM), Nanjing Tech University (NanjingTech), 30 South Puzhu Road, Nanjing 211800, China.

E-mail: iamjjshao@njtech.edu.cn

[b]Shaanxi Institute of Flexible Electronics (SIFE), Northwestern Polytechnical University (NPU), 127 West Youyi Road, Xi'an 710072, China

[c]School of Physical and Mathematical Sciences, Nanjing Tech University (NanjingTech), Nanjing 211800, China.

E-mail: iamxcdong@njtech.edu.cn

Supporting Information

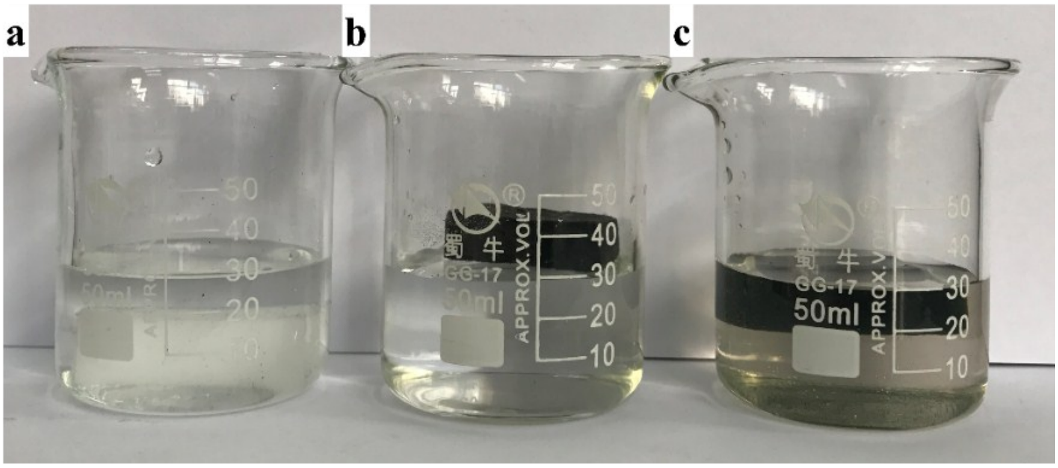

Figure S1. (a) Photograph of the hydrophilic pristine sponge. (b) Photograph of the hydrophobic RGS after rGO nanosheets were wrapped on the backbones. (c) Photograph of the hydrophilic RGPS when PANI NWs were *in-situ* synthesized on rGO nanosheets.

Supporting Information

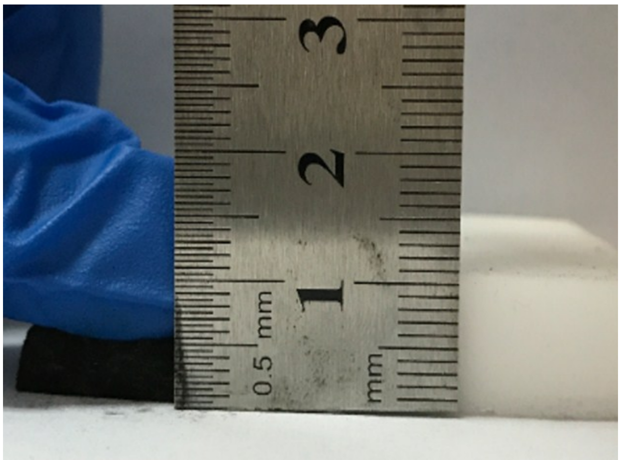

Figure S2. Photograph of the highly compressed (~50%) RGPS sponge.

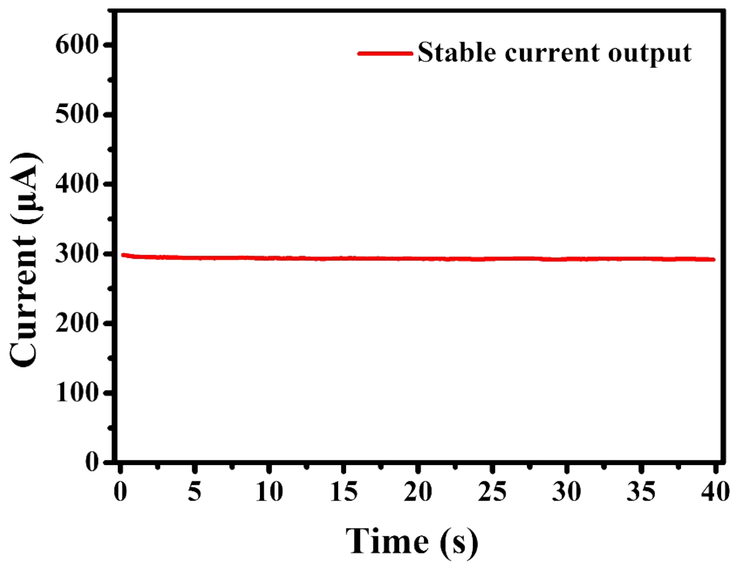

Figure S3. The stable current output signal of RGPS-4 based flexible sensor without pressure.

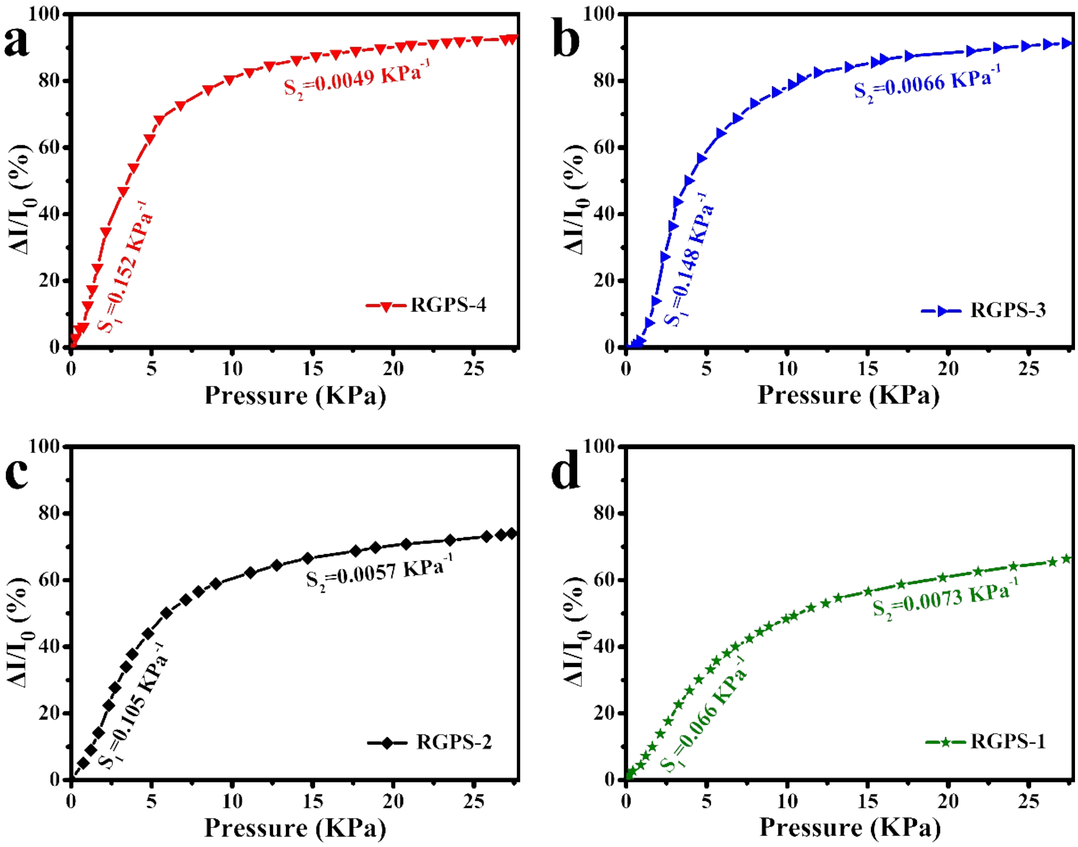

Figure S4. The pressure-sensing behavior of various sponges: (a) RGPS-4. (b) RGPS-3. (c) RGS-2. (d) RGPS-1.

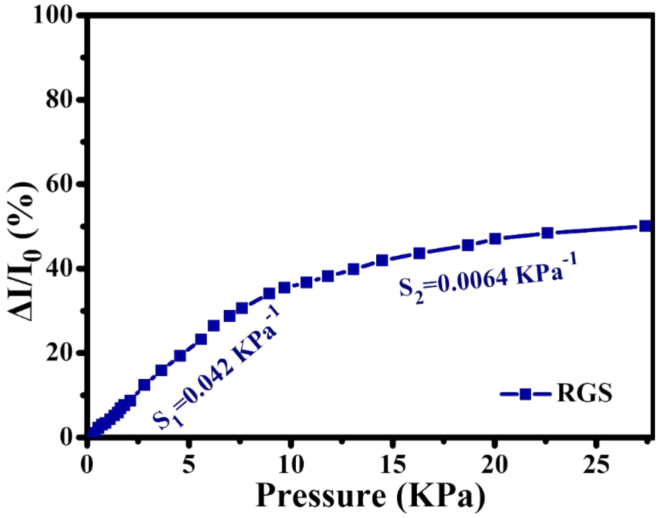

Figure S5. The piezoresistive performance of RGS based flexible sensor.

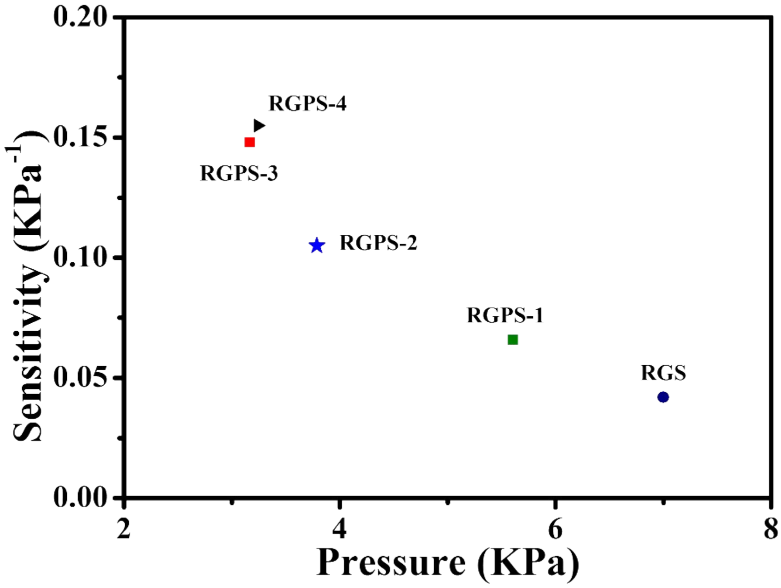

Figure S6. The piezoresistivity performance of various conductive sponges in the low pressure range. As shown in the illustration, the sensing behavior increases more slowly with increasing aniline concentration.

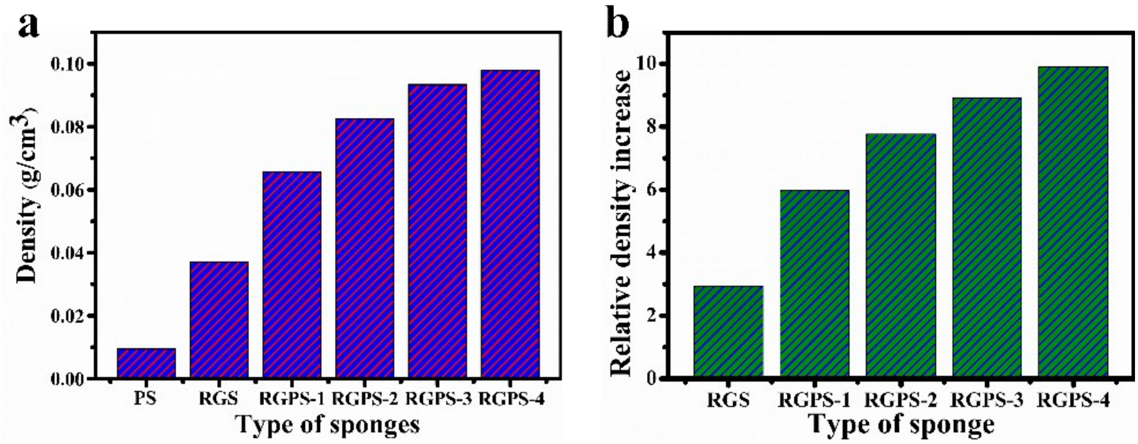

Figure S7. Illustrations of density (a) and relative density increase (b) of various sponges. PS refers to the pristine sponge.

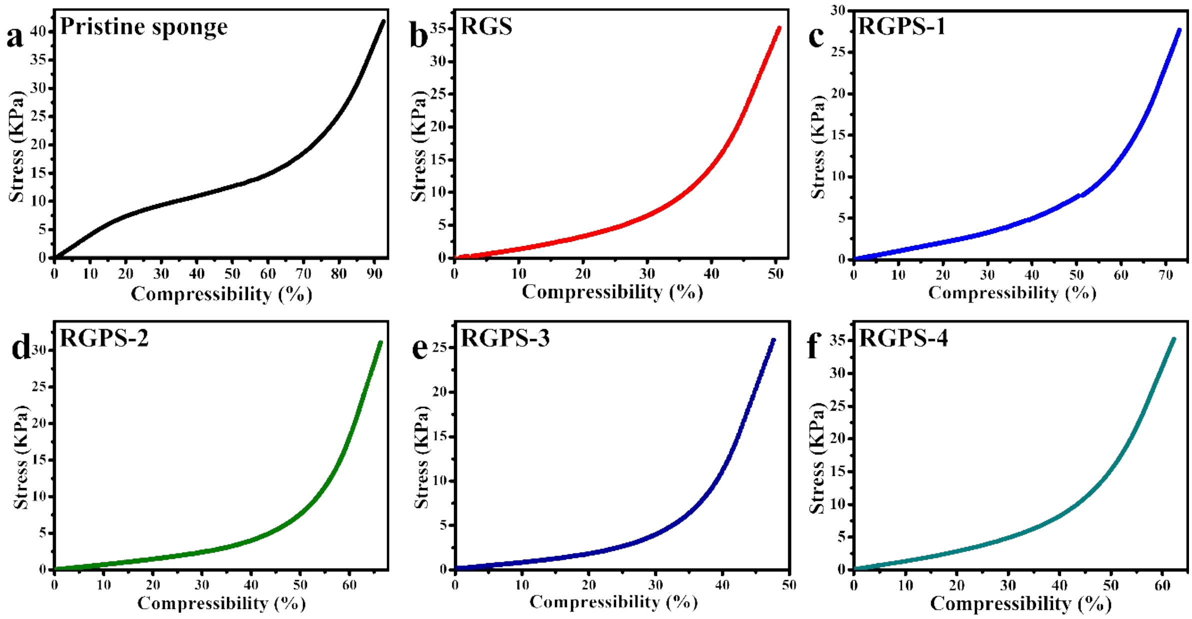

Figure S8. The measured mechanical property of various percolation networks based sensors. The curves in the above illustrations corresponded to pristine sponge (a), RGS (b), RGPS-1 (c), RGPS-2 (d), RGPS-3 (e), and RGPS-4 (f).

It could be found that the elastic modulus of different sponge deceases with the increasing loading amount of PANI NWs. Furthermore, the compressibility of different strain sensors also varies as micro-protruding PANI NWs were *in-situ* synthesized on building blocks, showing that the PANI coating can “soften” the rigid sponge.

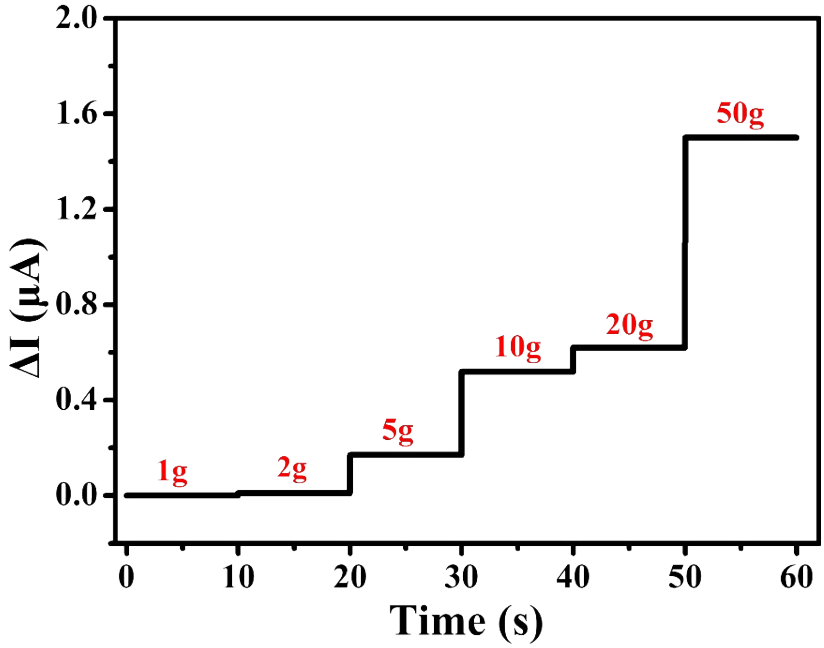

Figure S9. The real-time detection of the fabricated RGPS based flexible sensor when different loadings were exerted on the conductive sponge, showing that the current output increases with weights.

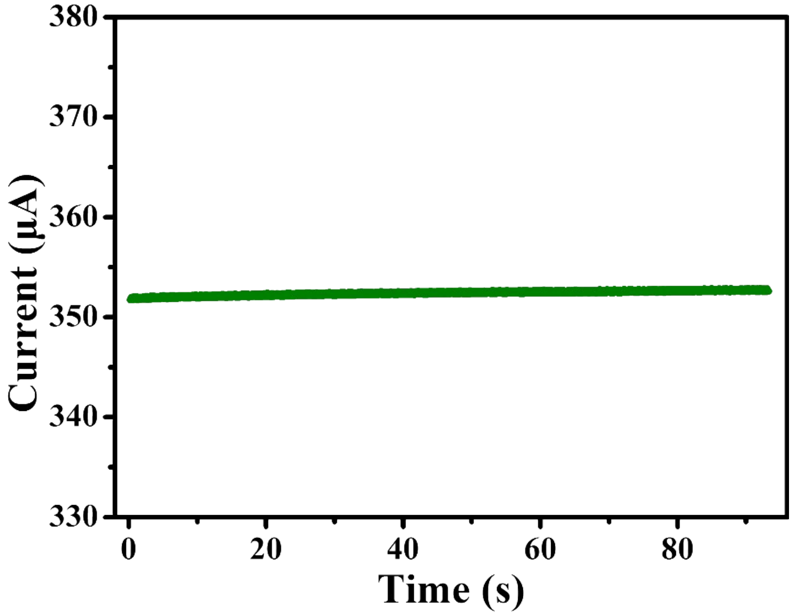

Figure S10. The ultra-stable current output signal of RGPS based flexible sensor after 9000 cycles of dynamic pressure deformations.

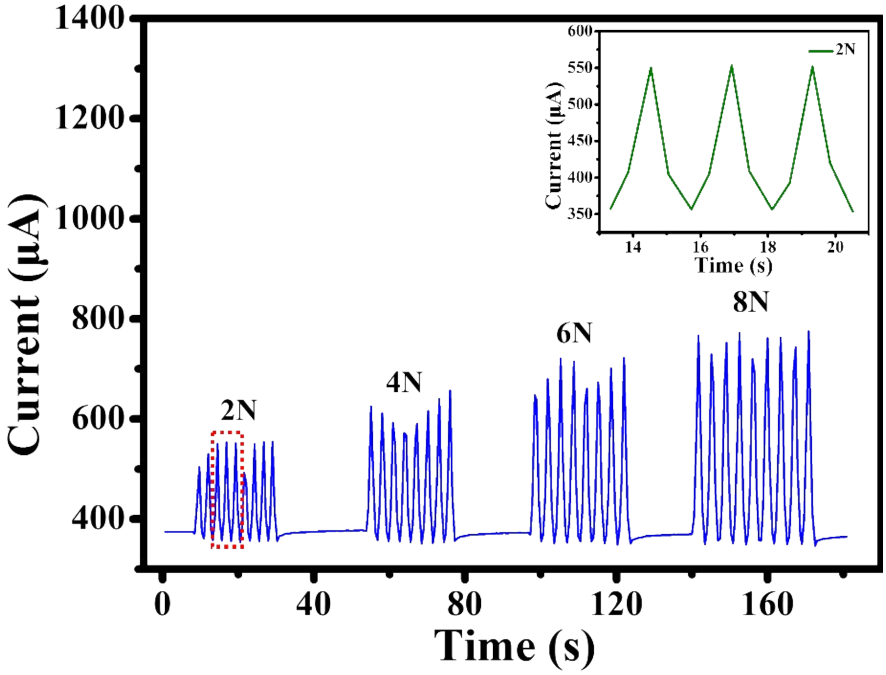

Figure S11. The piezoresistive performance of RGPS sponge after 9000 dynamic cycles. When different forces were exerted, the pressure sensor could distinguish different loadings and the signals were stable.

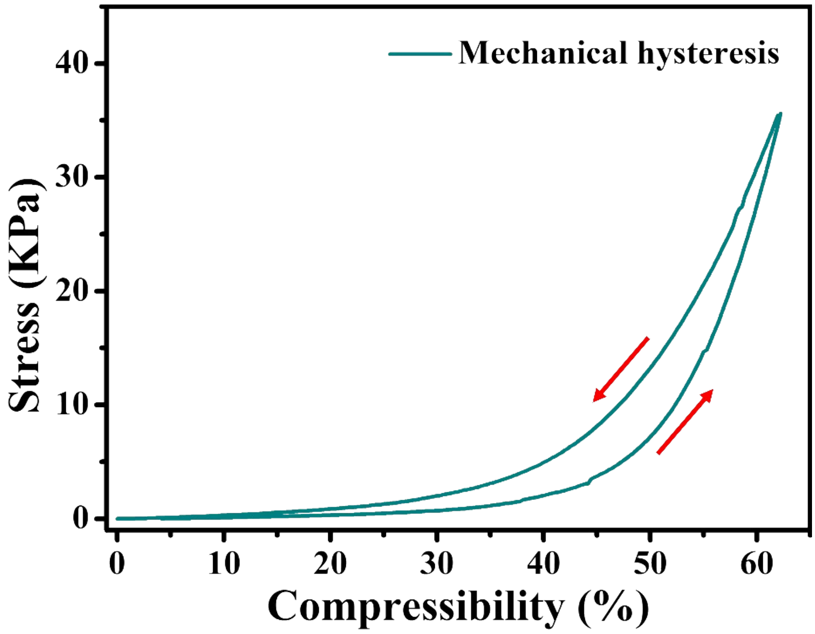

Figure S12. The mechanical hysteresis curve of RGPS based sensor after 9000 dynamic cycles. The maximum discrepancy between the loading and unloading curves was small, indicating the hysteresis problem in our sensor has been minimized.

Supporting Information

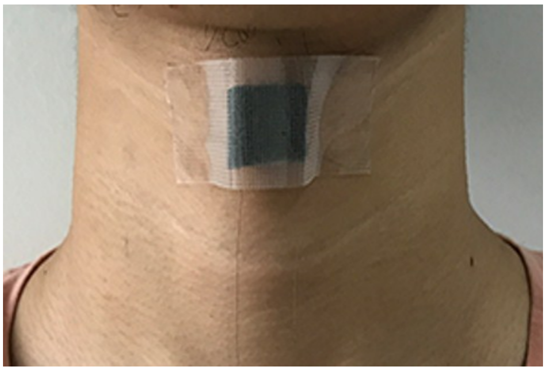

Figure S13. Photo showing how the pressure sensor can be used for sound sensing.

Supporting Information

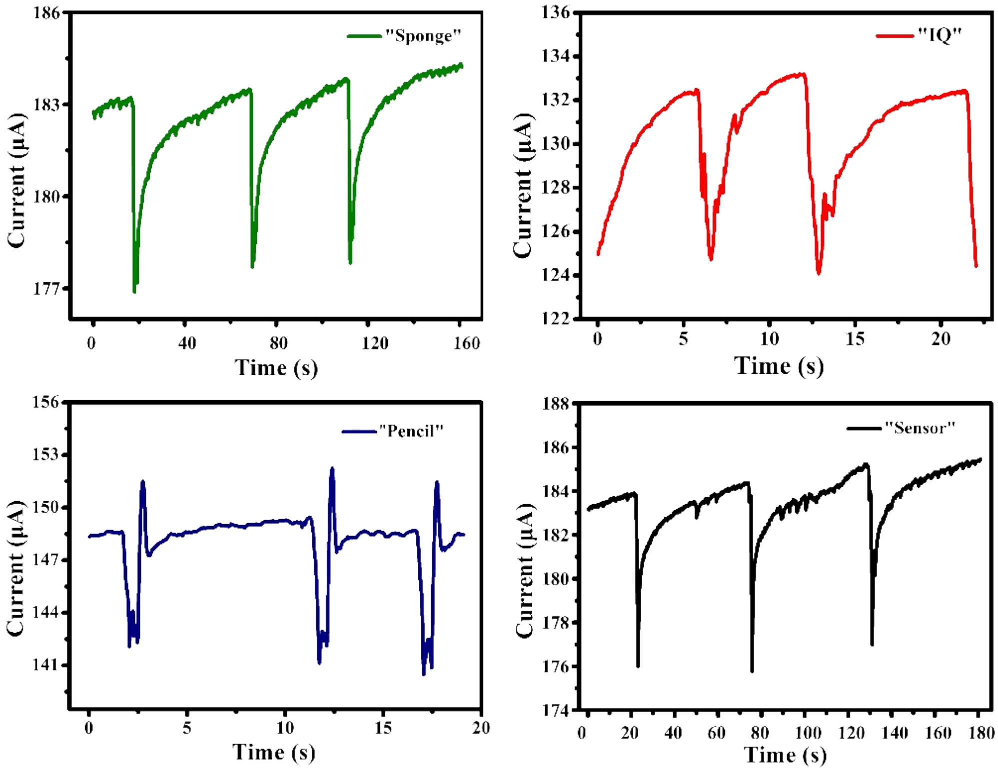

Figure S14. The detected current output signals of the flexible sensors when speaking "Sponge", "IQ", "Pencil" and "Sensor".

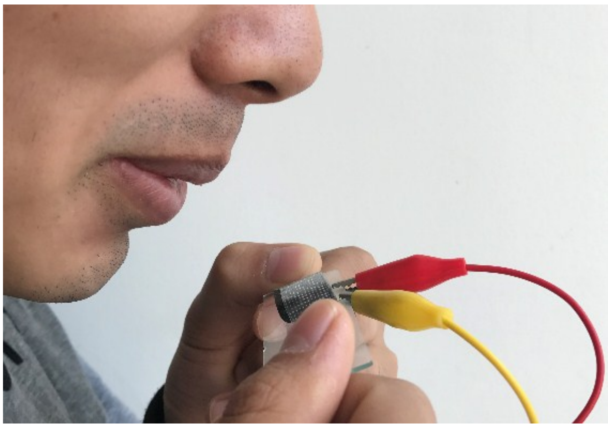

Figure S15. Photograph of the blowing process exerted on the RGPS based pressure sensor.

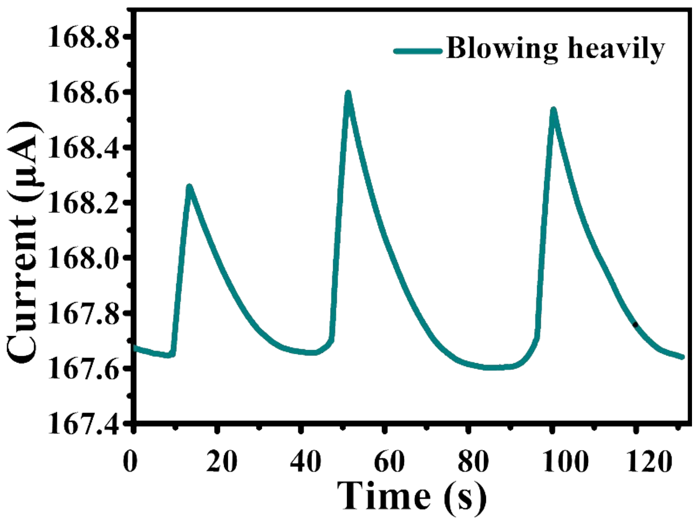

Figure S16. The corresponding current output during heavy blowing.

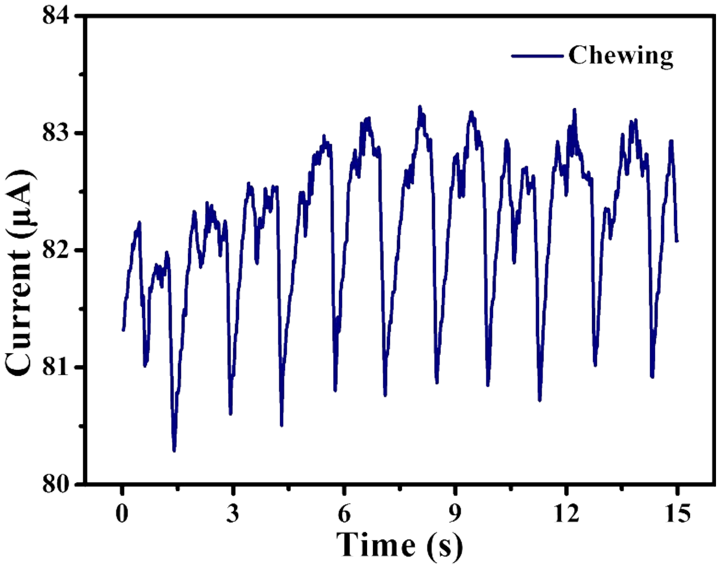

Figure S17. The current output signal of RGPS based sensor due to jaw motions when the volunteer chewed.